Dynamic Light Scattering Studies of Polymer Solutions. 5. Universal Behavior of Highly Swollen Chains at Infinite Dilution Observed for Polyisoprenes in Cyclohexane

Yoshisuke Tsunashima,* Masukazu Hirata, Norio Nemoto, and Michio Kurata

Institute for Chemical Research, Kyoto University, Uji, Kyoto-fu 611, Japan.
Received June 30, 1986

ABSTRACT: Dynamic behavior of narrow molecular weight distribution polyisoprenes in cyclohexane, a good solvent, at 25 °C has been investigated over small to intermediate qR_G region by means of homodyne photon correlation spectroscopy. The histogram method is employed for the analysis of the intensity autocorrelation function measured at various combinations of scattering vector q and polymer concentration c. The translational diffusion coefficient D, the effective decay rate (=the first cumulant) Γ_e, and the amplitude of the translational diffusion motion relative to that of the all molecular motions P_0/P have been determined as a function of q and c. The intrinsic values characterizing a single highly swollen chain have been obtained by extrapolating linearly the above-mentioned quantities to $c \to 0$ and/or to $q \to 0$. It has been found that polyisoprene chains are fairly well represented by the nondraining Gaussian chain model with nonpreaveraged Oseen hydrodynamic interaction. The apparent applicability of the Gaussian segment distribution function to the highly swollen polyisoprenes is interpreted in terms of the Domb–Gillis–Wilmer segment distribution function and the Fixman theory of the internal friction.

Introduction

In recent years, dynamical properties of isolated linear flexible chain molecules in dilute solutions have been studied extensively and have been discussed at more quantitative levels than were earlier. Experimental data have been accumulated mainly for polystyrenes (PS) which have long been regarded as the best model polymer of linear flexible chains. These data have revealed various discrepancies from the theoretical predictions in both Θ-solvents and good solvents, as demonstrated by the recent works of Han and Akcasu,[1] Tsunashima et al.,[2] and Nemoto et al.[3] When limited to the case of good solvents, the discrepancies are summarized as follows: (i) the molecular weight dependence of the translational diffusion coefficient at infinite dilution, $D_0 \propto M_w^{-0.55}$, was weaker than that of the root-mean-square radius of gyration, $R_G \equiv \langle S^2 \rangle_z^{1/2} \propto M_w^{0.60}$; (ii) the value of D_0 was smaller as compared with the theoretical estimates of Benmouna and Akcasu[4] by 16~19%; a 16% discrepancy was also observed for poly(methyl methacrylate) (PMMA) in good solvent;[5] (iii) at a sufficiently high q region defined by $b \ll q^{-1} \ll R_G$, where b is a statistical segment length and q the magnitude of $\boldsymbol{q}$, the experimental values of the first cumulant Γ_e showed the q^3 dependence which characterizes the nondraining chain, but the plateau values of Γ_e/q^3 lay below theoretical estimates of Benmouna and Akcasu[4] by about 30%. For these discrepancies, no satisfactory explanation has been given by the theories at present.

Turning to the experimental point of view, we found that PS and PMMA chains are much less flexible both statically and dynamically than are rubbery polymers such as polyisoprene (PIP) and polybutadiene (PB). Statically, this is assured by large values of the steric factor σ defined by the ratio of the mean-square end-to-end distances at the Θ-temperature to that of the free rotating chain, $\sigma \equiv (\langle R^2 \rangle_0 / \langle R^2 \rangle_{0f})^{1/2}$: $\sigma = 2.08 \pm 0.20$ (PMMA), 2.25 ± 0.05 (PS), 1.67 (*cis*-PIP), and $1.63 \sim 1.68$ (PB).[6] Dynamically, it is also assured by large values of the intrinsic dynamical viscosity $[\eta']_\infty$: $[\eta']_\infty = 22.8$ (PMMA), 14 (PS), $7 \sim 8$ (PIP), and 8 ± 2 (PB).[7] These values of $[\eta']_\infty$ were estimated as the frequency-independent value at extremely high frequency in the complex modulus vs. frequency plot. Thus, it is plausible that at least some part of the above-mentioned discrepancies between experiments and theories arises from insufficient chain flexibility in PS and PMMA. If so, dynamic light scattering measurements on rubbery polymers might help to explain these discrepancies.

In this paper, therefore, we selected PIP as a model rubbery polymer and have studied its dynamic light scattering behavior in cyclohexane, a good solvent, over an extended region of qR_G as previously done by us for PS in benzene.[3] Then we have tried to obtain the generalized dynamical scheme of a single highly swollen chain in dilute solutions from the purely experimental point of view. In this scheme, how the hydrodynamic interaction operates on the chain monomers has been investigated.

Experimental Section

Materials. The PIP samples were prepared by Dr. D. Nerger, by anionic polymerization in benzene, and fractionated by his group by methods described earlier by others.[8,9] These samples became available for the present study through the courtesy of Dr. K. Kajiwara of our Institute. Five samples, coded as L-14, L-12, L-15, L-11, and L-16, covered the molecular weight region from 0.326×10^6 to 7.24×10^6, and the homogeneity of each sample was guaranteed as $M_w/M_n \leq 1.1$ by sedimentation velocity profiles obtained in this laboratory. Cyclohexane (spectrograde, Nakarai Chemicals, Kyoto) was used as a good solvent without further purification. The refractive index, density, and viscosity of cyclohexane were estimated to be $n = 1.4285$ (488 nm) and 1.4220 (633 nm), $d = 0.77394$ g cm^{-3}, and $\eta_0 = 0.898 \times 10^{-2}$ g cm^{-1} s^{-1}, respectively, at 25 °C from literature values.[10] Polymer solutions at various concentrations were prepared by mixing by weight the pure solvent and a polymer solution of known concentration. They were freed from dust by filtration (Millipore filters) for all the samples except the highest molecular weight one, to which centrifugation (preparative, temperature-controlled Type 55P, Hitachi Ltd.) was applied. All the preparation procedures were carried out in dryboxes under N_2 atmosphere. No antioxidant was added in the solutions. Preliminary static and dynamic light scattering measurements were carried out on both antioxidant-free and -added (0.05 wt % 2,6-di-*tert*-butyl-*p*-cresol) solutions to confirm that no oxidative degradation took place during measurements.

The static characterization of these polymer samples in cyclohexane was carried out with a light scattering photometer (Unisoku, Hirakata; modified by us) at 25.0 ± 0.02 °C. The vertically polarized light scattered from the solution illuminated with a vertically polarized He–Ne laser (633 nm) was measured. The scattering angles were changed from 10° to 150° at intervals of 2–5°. The specific refractive index increment of PIP in cyclohexane at 25 °C for 633 nm was taken to be 0.106 cm^3 g^{-1}, the value reported by Hadjichristidis and Fetters.[11] Absolute calibration of the photometer was made with benzene (spectrograde, Nakarai Chemicals), for which the absolute Rayleigh ratio due

0024-9297/87/2220-1992$01.50/0

Table I
Characteristics of Polyisoprenes in Cyclohexane at 25 °C

sample	$10^{-6}M_w$	R_G, 10^{-6} cm	A_2, 10^{-4} mol cm^3 g^{-2}	microstructure,[a] mol % cis-1,4	trans-1,4	3,4
L-14	0.326	3.16	8.04	73.3	21.9	4.8
L-12	0.568	4.33	7.03	67.0	25.3	7.7
L-15	0.578	4.35	6.77	68.6	24.7	6.7
L-11	2.44	10.5_0	4.74	84.1	11.9	4.0
L-16	7.24	21.0_2	4.37	86.7	10.3	3.0

[a] Measured in $CDCl_3$ at 35 °C.

to Pike et al.[12], R_{U_v} (90) = 11.84 × 10^{-6} cm^{-1} (633 nm), was employed.

The microstructure of PIP was examined in $CDCl_3$ (3 w/v %) at 35 °C with a 400-MHz ^{1}H NMR spectrometer (Japan Electron Optics Laboratory, JNM-GX 400) installed in Kitamaru's Laboratory of this Institute. The signal assignments were made on the basis of the data reported by Tanaka et al.[13] The characteristics of the PIP samples thus determined are summarized in Table I.

Dynamic Light Scattering. Dust-free solutions of PIP in cyclohexane were prepared by the same procedure applied to solutions for static light scattering. With an instrument described earlier,[14] the intensity autocorrelation function $A(\tau)$ of the solution was measured at 25.0 ± 0.02 °C by either a time interval correlator (made in our laboratory, 512 channels)[14] or a shift register correlator (Malvern, 72 channels). The incident light was a vertically polarized single-frequency 488-nm line emitted from an argon ion laser (Spectra Physics, Model 165–03) with a space etalon. The photomultiplier tube (Hamamatsu Photonics, R464-C1050) was set at six fixed scattering angles at 10°, 30°, 60°, 90°, 120°, and 150° to detect the vertical component of the scattered light from the solutions. The $A(\tau)$ data were analyzed by the histogram method[15] with a nonlinear least-squares algorithm. A FACOM M180IIAD computer in our Institute was used for the analysis.

Sedimentation Velocity. The sedimentation velocity of solutions was measured in an analytical ultracentrifuge (Beckman, Spinco Model E) at 25.0 ± 0.1 °C and rotor speed of 42040 or 59780 rpm with use of a single sector cell 12 mm long. The Schlieren diagrams obtained were read on a contour projector (Nihon Kogaku).

Data Analysis, Evaluation of Dynamic Characteristics, and Results

Dynamic Light Scattering. The translational diffusion coefficients at finite polymer concentration, $D(c)$, for four samples other than the highest molecular weight sample L-16 were estimated by fitting the $A(\tau)$ data in the region, qR_G ($\equiv X^{1/2}$) < 0.4, to a single-exponential decay curve. For sample L-16, the histogram analysis was applied. The analysis gave a sharp unimodal distribution of the decay rate, Γ, at the scattering angle θ = 10° (X = 0.454). The diffusion coefficient, $D(c)$, was evaluated from the effective decay rate, $\Gamma_e(c)$ [$=D(c)q^2$]. This $D(c)$ value agrees to within about 3% with the value evaluated from the slow component of a bimodal Γ distribution which was obtained at the next smallest angle, θ = 30° (X = 4.01). Figure 1 shows the $D(c)$ values for all five samples as functions of concentration, c. All the data points are well represented by the linear relation

$$D(c) = D_0(1 + k_D c) \quad (1)$$

which yields D_0 and k_D listed in Table II.

The first cumulants (or the effective decay rate), $\Gamma_e(q,c)$, at given q and c were estimated by averaging Γ over either a bimodal distribution $G(\Gamma)$ for X < 10 or a broad unimodal one for X > 10. Figure 2 shows an example of the concentration dependence of $\Gamma_e(q,c)$ at constant q obtained for solutions of L-16. The data for each q are well represented by equations linear in c, as shown in Figure 2,

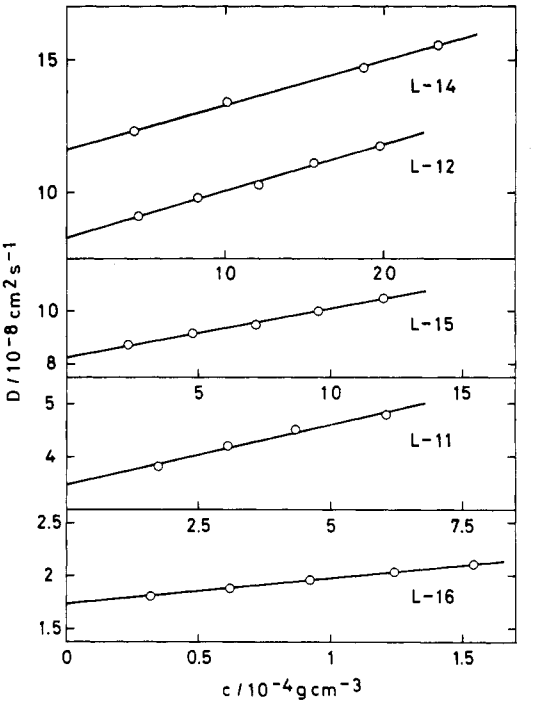

Figure 1. Concentration dependence of the translational diffusion coefficients, D, obtained for five PIP samples in cyclohexane at 25 °C.

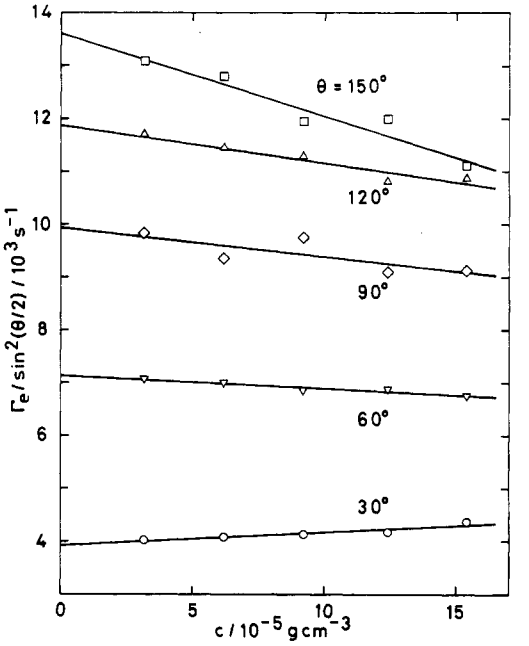

Figure 2. Linear extrapolation of the reduced effective decay rates, $\Gamma_e(q,c)/\sin^2(\theta/2)$, obtained for the solutions of the highest molecular weight sample L-16 to infinite dilution at five scattering angles from 30° to 150°.

Table II
Experimental Results of D_0, s_0, k_D, k_s, and $\bar{v}$ Obtained for Polyisoprenes in Cyclohexane at 25 °C

sample	D_0, 10^{-8} cm^2 s^{-1}	s_0, 10^{-13} s	k_D, cm^3 g^{-1}	k_s, cm^3 g^{-1}	$\bar{v}$, cm^3 g^{-1}
L-14	11.66	2.09	142	319	1.116
L-12	8.29_3	2.70	217	482	1.109
L-15	8.27_1	2.77	221	522	1.107
L-11	3.47_6	4.79	651	1320	1.111
L-16	1.73_7	7.24	1390	3260	1.108

from which the infinite dilution values $\Gamma_e(q,0)$ are estimated. The slopes change sign from positive to negative

Table III
Experimental Results of Effective Decay Rate (=First Cumulant) for Polyisoprenes in Cyclohexane at 25 °C

angle, deg	X	$\Gamma_e(q,0)/q^2$, 10^{-8} s^{-1}
	L-16	
150	55.80	10.06
120	44.85	8.78
90	29.90	7.35
60	14.95	5.28
30	4.006	2.89
10	0.454 3	1.74
$\theta \to 0$	0.0	1.73_7
	L-12	
150	2.367	12.19
120	1.903	11.60
90	1.269	10.20
60	0.634 2	
30	0.169 9	8.29
10	0.019 27	
$\theta \to 0$	0.0	8.29_2
	L-11	
150	13.92	9.98
120	11.19	9.02
90	7.458	7.46
60	3.729	5.76
30	0.999 2	4.21
10	0.113 3	3.47
$\theta \to 0$	0.0	3.47_6
	L-15	
30	0.171 5	8.27
10	0.019 45	
$\theta \to 0$	0.0	8.27_0
	L-14	
30	0.090 51	11.66
10	0.010 26	
$\theta \to 0$	0.0	11.66

values with increasing $X^{1/2}$, as was the case for PS in benzene.[3] For $q \ll 1$, the $\Gamma_e(q,0)$ value becomes equivalent to D_0q^2, as it should. Table III shows the q dependence of $\Gamma_e(q,0)$ values thus obtained for the five samples. The increase of $\Gamma_e(q,0)/q^2$ with q, which reflects internal motions, was analyzed at small X by

$$\Gamma_e(q,0)/q^2 = D_0[1 + C(t = 0)X + ...] \quad (2)$$

from which the dimensionless parameter C was estimated.[16]

The amplitude of the translational diffusion mode relative to the total mode, $P_0(X)/P(X)$, was estimated from the fractional area of the slow component in the bimodal Γ distribution that was obtained by analyzing the $A(\tau)$ data for given c and X in the range $1.5 < X < 10$. Here, $P_0(X)$ and $P(X)$ are the particle scattering functions for the translational and the total motion, respectively. The concentration dependence of P_0/P thus estimated for L-16, L-12, and L-11 is shown in Figure 3. For each sample, the P_0/P at given q depends linearly on c, as shown by the solid lines in the figure. Table IV gives the infinite dilution values $(P_0/P)_{c\to 0}$. The slope of the solid lines in Figure 3 increases with increasing X, irrespective of the sample molecular weight. The values of $d(P_0/P)/dc$ are also included in Table IV.

Sedimentation Velocity. The sedimentation coefficients at finite polymer concentrations $s(c)$ were estimated by fitting the movement of the sedimentation boundary to the Billick–Fujita equation:[17,18]

$$\ln (r/r_m)/\omega^2(t - t_0) = s(c)\{1 + B[(r/r_m)^2 - 1]\} \quad (3)$$

Here r and r_m are the radical distances of the sedimentation boundary and the meniscus from the rotation axis, ω is the angular velocity, t is the time measured from the moment when the rotor is set in motion, and B is a constant relating to the pressure effect on $s(c)$. The zero-time correction t_0 for the acceleration period was determined in such a way that plots of $\ln (r/r_m)/\omega^2(t - t_0)$ vs. $(r/r_m)^2 - 1$ became linear over as wide a range of the abscissa as possible.[19,20] Figure 4 shows the concentration dependence of $1/s(c)$ thus obtained. The data points for each sample are well represented by the linear relation

$$1/s(c) = (1/s_0)(1 + k_s c) \quad (4)$$

which yield s_0 and k_s listed in Table II.

The s_0 must satisfy the well-known equation

$$D_0M/s_0 = RT/(1 - \bar{v}d) \quad (5)$$

where R is the gas constant, M and $\bar{v}$ are the molar mass and the partial specific volume of the polymer, and d is the solvent density. Thus, using the experimental values of M_w, D_0, and s_0, we can evaluate $\bar{v}$ of each PIP sample as shown in the last column of Table II. The average value, $\bar{v} = 1.110 \pm 0.003$ cm^3 g^{-1} at 25 °C, is favorably compared with the literature value, 1.10 cm^3 g^{-1}, for a natural rubber in cyclohexane at 20 °C.[21] (We did not measure $\bar{v}$ in this study.)

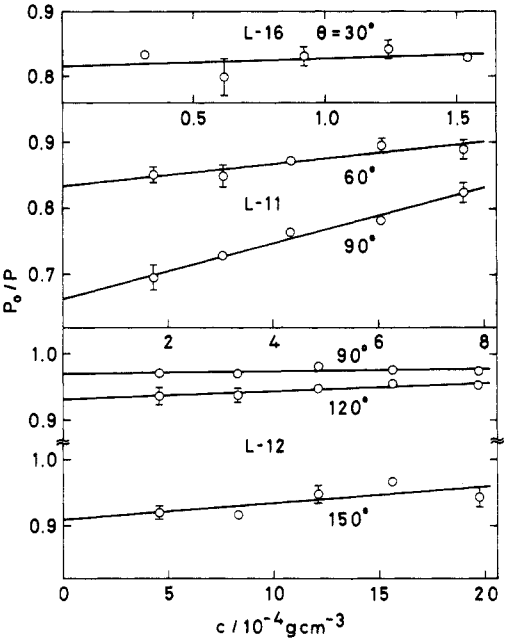

Figure 3. Linear extrapolation of the relative amplitudes, P_0/P, to infinite dilution; from top to bottom, the solution of L-16 at the scattering angle $\theta = 30°$; L-11 at $\theta = 60°$ and 90°; L-12 at $\theta = 90°$, 120°, and 150°.

Table IV
Experimental Results of Relative Amplitude of Translational Diffusion Motion $(P_0/P)_{c\to 0}$ for Polyisoprenes in Cyclohexane at 25 °C

sample	X	$(P_0/P)_{c\to 0}$	$d(P_0/P)/dc$, cm^3 g^{-1}
L-12	1.269	0.970	0.0003
	1.903	0.931	0.0013
	2.367	0.909	0.0025
L-11	3.729	0.834	0.0082
	7.458	0.663	0.021
L-16	4.006	0.816	0.012

Discussion

Molecular Weight Dependence of Static Characteristics. Figure 5 shows the molecular weight depen-

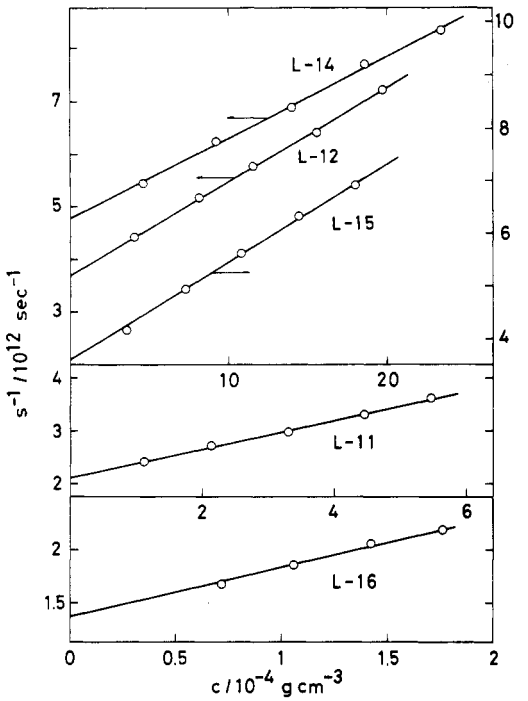

Figure 4. Concentration dependence of the inverse sedimentation coefficients, s^{-1}, obtained for five PIP samples in cyclohexane at 25 °C.

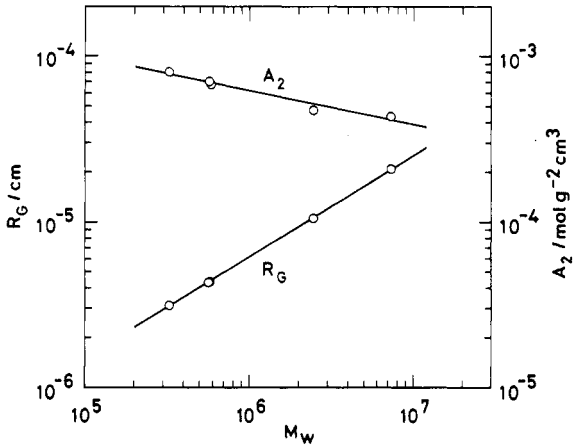

Figure 5. Logarithmic plots of the root-mean-square radius of gyration, R_G, and the second virial coefficient, A_2, against the weight-average molecular weight, M_w, obtained for five PIP samples in cyclohexane at 25 °C.

dences of R_G and A_2 (the second virial coefficient for static light scattering) on logarithmic scales. The data are well represented by

$$R_G = 1.35 \times 10^{-9} M_w^{0.61\pm0.01} \quad \text{(cm)} \tag{6}$$

$$A_2 = 9.80 \times 10^{-3} M_w^{-0.20\pm0.02} \quad \text{(mol cm}^3\text{ g}^{-2}\text{)} \tag{7}$$

respectively. The exponents ν in these equations are in agreement, to within experimental error, with the theoretical asymptotic values obtained for linear flexible polymers in good solvents, i.e., $\nu_{R_G} = 0.6$ and $\nu_{A_2} = -0.2$.[22] It is thus confirmed that, in the molecular weight region examined in the present work, PIP behaves as highly swollen chains in the static sense. This is notable as compared with PS, of which ν_{A_2} attains the asymptotic value −0.2 at higher molecular weights, say $M_w > 2 \times 10^7$.[23,24]

Molecular Weight Dependence of Diffusion and Sedimentation Coefficients. The molecular weight dependence of D_0 and s_0 is shown in Figures 6 and 7, respectively. These data are well represented by

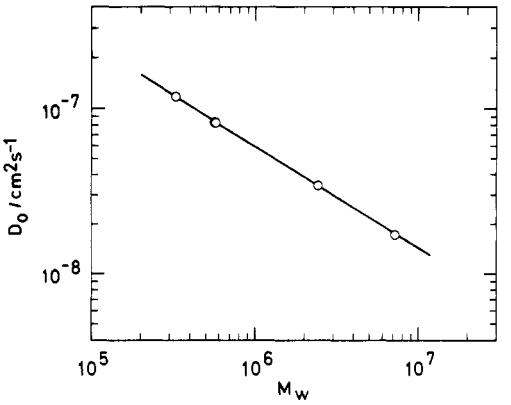

Figure 6. Logarithmic plot of the translational diffusion coefficient at infinite dilution, D_0, against M_w obtained for PIP in cyclohexane at 25 °C.

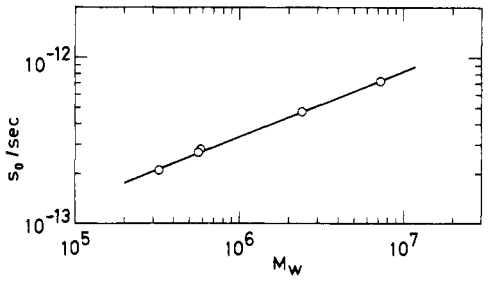

Figure 7. Logarithmic plots of the sedimentation coefficient at infinite dilution, s_0, against M_w obtained for PIP in cyclohexane at 25 °C.

Table V
Equivalent Hydrodynamic Radius R_H and Dimensionless Parameter ρ ($=R_G/R_H$) for Polyisoprenes in Cyclohexane at 25 °C

	sample				
	L-14	L-12	L-15	L-11	L-16
R_H,[a] 10^{-6} cm	2.08_6	2.93_3	2.94_0	6.99_7	14.0_0
ρ	1.51	1.48	1.48	1.50	1.50

[a] R_H was calculated from the relation $R_H = k_B T/6\pi\eta_0 D_0$.

$$D_0 = 2.69 \times 10^{-4} M_w^{-0.61\pm0.01} \quad \text{(cm}^2\text{ s}^{-1}\text{)} \tag{8}$$

$$s_0 = 1.43 \times 10^{-15} M_w^{0.395\pm0.01} \quad \text{(s)} \tag{9}$$

respectively. Two exponents in these equations satisfy the relationship, $\nu_{s_0} - \nu_{D_0} = 1$, as is expected from eq 5, and indicate that PIP behaves as highly swollen chains in the dynamic sense too.

Stokes Radius. Equation 8 can be rewritten in terms of the equivalent Stokes radius R_H of a polymer as

$$D_0 = k_B T/6\pi\eta_0 R_H \tag{10}$$

$$R_H = 9.03 \times 10^{-10} M_w^{0.61\pm0.01} \quad \text{(cm)} \tag{11}$$

Here η_0 represents the solvent viscosity and k_B the Boltzmann constant. The ratio, $\rho = R_G/R_H$, obtained for each polymer sample is constant, to within experimental error, as shown in Table V.

According to Kirkwood[25] and also to Akcasu and Gurol,[26] the Stokes radius, R_H, can be expressed as

$$R_H^{-1} = N^{-2} \sum_{i=1}^{N} \sum_{j=1}^{N} \langle 1/r_{ij} \rangle \qquad i \neq j \tag{12}$$

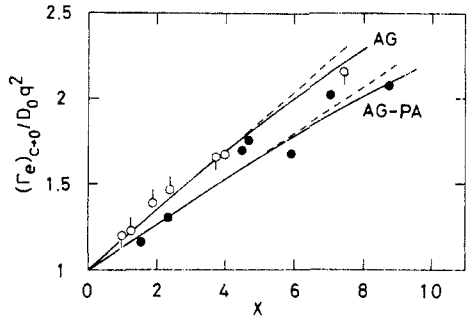

Figure 8. Reduced values of $\Gamma_e(q,0)/D_0q^2$ plotted against X in the small range $X < 8$: (○) L-16, (♀) L-11, (♁) L-12 for PIP in cyclohexane at 25 °C; (●) PS data in benzene at 30 °C.[3] The solid lines AG and AG-PA are the theoretical curves calculated by Akcasu and Gurol[16,26] for the nondraining Gaussian chains with preaveraged (PA) and non-PA Oseen hydrodynamic interaction, respectively, and the corresponding broken lines represent the initial slope, 2/15 and 13/75, respectively.

in the long-chain, nondraining limit. The corresponding expression for the radius of gyration, R_G, is

$$R_G^2 = (1/2N^2)\sum_{i=1}^{N}\sum_{j=1}^{N}\langle r_{ij}^2\rangle \qquad i \neq j \tag{13}$$

where N represents the number of chain elements in a molecule and r_{ij} the spatial distance between elements i and j. Equations 12 and 13 lead to the well-known theoretical value, $\rho = 1.504$, for the Gaussian chain,[26] which is in good agreement with the experimental values, ca. 1.50, in Table V. However, this agreement is fortuitous, for the PIP chains are not Gaussian.

We have recently found in the study of static scattering function for highly swollen polymers[27] that the distribution function for r_{ij} is well represented by the generalized Domb–Gillis–Wilmers function[28]

$$W(r,n) = C_n r^l \exp[-(r/\sigma_n)^t] \quad (n \equiv |i-j|,\ r \equiv r_{ij}) \tag{14}$$

with critical indexes, $t = 2.40$ and $l = 2.80$. Here C_n is the normalization constant and σ_n is the scaling factor, respectively. If eq 14 is adopted in the calculation of R_H and R_G, we obtain $\rho = 1.596$ as shown in the Appendix section, which yields $\rho_{exptl}/\rho_{calcd} = 0.94$. This value is to be compared with 0.85 obtained in Θ-solvents.[29] If we interpret these results in terms of the recent theory of Fixman,[30] the strength of *internal friction* λ decreases with increasing expansion of polymer coils.

In this connection, it may be pertinent to note that Benmouna and Akcasu[4] have obtained $\rho_{calcd} = 1.860$ for highly swollen chains with $\nu_{R_G} = {}^3/_5$ by using Ptitsyn's pseudo-Gaussian form (or the blob model form) of $W(r,n)$, i.e., eq 14 with $t = l = 2$. This value of ρ_{calcd} gives $\rho_{exptl}/\rho_{calcd} = 0.81$ and hence predicts the change of λ in the opposite direction to the above. Thus, we may reconfirm the significance of the dangling chain effect on the short-range behavior of W, which is represented by the high value of l.[31]

First Cumulant—Small-q Region. Figure 8 shows the X ($=q^2R_G^2$) dependence of $\Gamma_e(q,0)/D_0q^2$ in the small range $X < 8$. The notation $(\Gamma_e)_{c\to 0}$ in the ordinate denotes $\Gamma_e(q,0)$. Irrespective of molecular weight, the PIP data shown by unfilled circles are located near the solid line AG or the theoretical curve obtained by Akcasu and Gurol[26] for nondraining *Gaussian* chains with nonpreaveraged (non-PA) Oseen hydrodynamic interaction. The broken line or the initial slope of the curve AG represents the already mentioned dimensionless parameter $C(t = 0)$ in eq 2 and gives[16] $C = 13/75 = 0.173$.

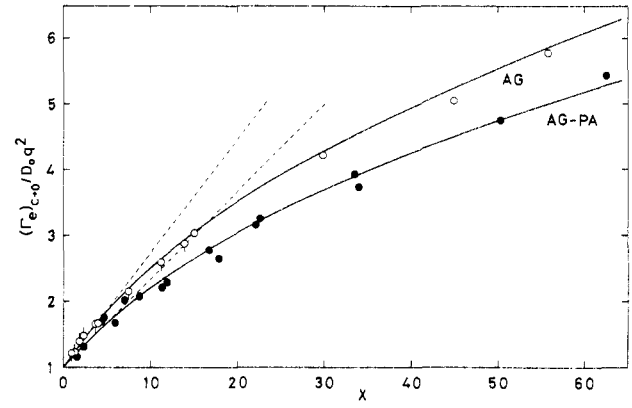

Figure 9. Reduced values of $\Gamma_e(q,0)/D_0q^2$ plotted against X in the large range of $0 < X < 65$. Symbols are the same as in Figure 8.

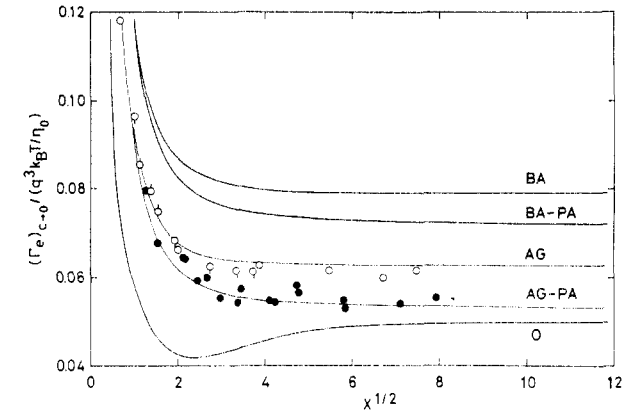

Figure 10. Plot of the reduced effective decay rate $\Gamma_e(q,0)/(q^3k_BT/\eta_0)$ against $X^{1/2}$: (○) L-16, (♀) L-11, (♁) L-12 for PIP in cyclohexane at 25 °C; (●) PS data in benzene at 30 °C. Various lines are the theoretical curves calculated for the nondraining flexible coil: BA and BA-PA are Benmouna–Akcasu calculation with non-PA[4,34] and PA[36] Oseen tensor, respectively, in good solvent limit; AG and AG-PA are Akcasu–Gurol one with non-PA and PA, respectively, in Θ-state[26]; (O) is self-avoiding chain with non-PA Oseen tensor.[37]

In Figure 8, we show also our previous data[3] for PS in benzene by the filled circles. The data, though considerably scattered, seem to favor the solid line AG-PA for the nondraining Gaussian chains with preaveraged (PA) Oseen interaction, of which the initial slope gives $C = 2/15 = 0.133$.[16] However, Bantle et al.[32] have reported that their data for a PS sample with molecular weight, $M_w = 2.89 \times 10^6$, yield C value of ca. 0.2.

According to Tanaka and Stockmayer,[33] the quantity C depends to a negligible extent on the excluded volume effect within the first-order perturbation treatment. For highly swollen chains, however, the theoretical value of C has not been established yet. (Following the Han–Akcasu scheme,[1] we could obtain $C \approx 0.175$ for PA hydrodynamic interaction.) Here we simply note that the dynamic behavior of highly swollen chains in the small-q region is fairly well described by the Akcasu–Gurol theory for Gaussian chains.

First Cumulant—Intermediate-q Region. Figure 9 shows the X dependence of $\Gamma_e(q,0)/D_0q^2$ in the extended range $X < 65$, where unfilled circles are the present data on three PIP samples in cyclohexane and the filled circles are our previous data[3] on four PS samples in benzene. To our surprise, the PIP data are still well represented by the Akcasu–Gurol curve for nondraining Gaussian chains with non-PA[16,26] over the wide range of X, while the PS data are well represented by the AG-PA curve.

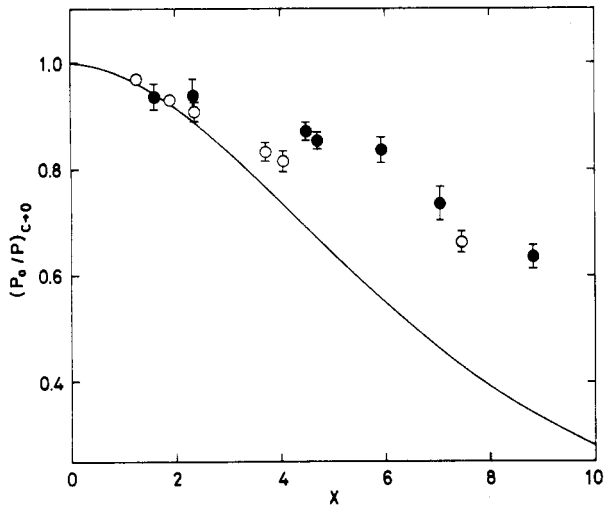

Figure 11. Dependence of the amplitude of translational diffusion motion relative to that of all molecular motions $(P_0/P)_{c\to 0}$ against X: (○) present data for PIP in cyclohexane at 25 °C; (●) PS data in benzene at 30 °C.[3] The solid curve is a theoretical one for the nondraining Gaussian chain with the PA Oseen tensor.[38,39]

Figure 10 shows the plot of the reduced first cumulant $\Gamma_e(q,0)/(q^3k_BT/\eta_0)$ against $X^{1/2}$, where unfilled and filled circles represent PIP and PS data, respectively. The experimental data on PIP produce a master curve irrespective of molecular weight, which decreases rapidly with increasing $X^{1/2}$ for $X^{1/2} < 2$ and then approaches asymptotically a constant in the range $X^{1/2} > 4$. The constancy of $\Gamma_e(q,0)/q^3$ confirms the nondraining nature of the PIP chains. The thin solid line AG[26] and the thick solid line BA[4,34] in Figure 10 represent theoretical curves which were obtained for nondraining chains with nonpreaveraged Oseen tensor in the Θ-state and in the highly swollen state, respectively. Their asymptotic values are 0.0625 for AG and 0.0788 for BA, respectively. It is obvious that the PIP data fit the AG curve rather than the BA curve. The situation resembles the one encountered in the case of Stokes radius. It has already been revealed[35] that the pseudo-Gaussian distribution function (eq 14 with $l = t = 2$) employed in the BA calculation is not a good choice for predicting correctly the behavior of static scattering function in the intermediate-q region $X^{1/2} > 2$. Effect of the precise form of segment distribution function on Γ_e still remains unclear. We have no explanation for the above observation on Γ_e.

We show in Figure 10 the asymptotic values of $\Gamma_e(q,0)/(q^3k_BT/\eta_0)$ for chains with preaveraged Oseen tensor by solid lines AG-PA[26] and BA-PA.[36] We show also another theoretical curve O which was obtained by Oono[37] for nondraining self-avoiding (swollen) chains with nonpreaveraged Oseen tensor. Reading off the asymptotic $\Gamma_e/(q^3k_BT/\eta_0)$ of his drawings, we obtain 0.050 for swollen chains and 0.027 for Gaussian chains. However, it is beyond our task to comment on these figures.

Relative Amplitude of Translational Diffusion Motion. In Figure 11, the X dependence of the relative amplitude of translational motion at infinite dilution $(P_0/P)_{c\to 0}$ is shown, where the unfilled circles represent the present data, the filled circles our previous data for PS in benzene,[3] and the solid line the theoretical curve for nondraining Gaussian chains with PA Oseen tensor.[38,39] The non-PA curve of $(P_0/P)_{c\to 0}$ has not been presented. With the increase of X, the $(P_0/P)_{c\to 0}$ for PIP decreases along the solid curve in the range $X < 3$ and then deviates from the curve upward in $X > 3$. It has been widely recognized that the static scattering function $P(X)$ for swollen chains is well represented up to $X \cong 10$ by the Debye function for Gaussian chains.[23,35] In other words, the uniform expansion approximation for the segment distribution function is effective up to $X \cong 10$ in the case of $P(X)$ and also of Γ_e. The deviation of experimental P_0/P from the Gaussian curve at small X may be a source of information on the precise form of the segment distribution function. Since the separation of the diffusion mode P_0 can be performed with reasonable precision by the histogram method,[39] we do not think the deviation to be artificial. To test this conjecture, we need a theory of P_0.

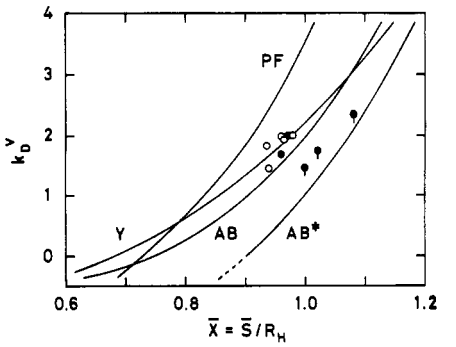

Figure 12. Volume-fraction frame, k_D^V, plotted against parameter $\bar{X}$, which represents a ratio of the radius of equivalent thermodynamic sphere, $\bar{S}$, to that of equivalent hydrodynamic sphere, R_H, in the $\bar{X}$ range of good solvent atmosphere: (○) present data for PIP in cyclohexane; (●) data for PS in benzene[3] in $M_w < 4 \times 10^6$; (◐) data for PS in benzene[3] in $M_w > 4 \times 10^6$. The solid lines Y, AB, and PF are the theoretical curves shown in eq 15, 16, and 17, respectively, and AB* is expressed by the relation, $k_D^V(AB^*) = k_D^V(AB) - 1$.

Concentration Dependence of D. As compared with the infinite dilution characteristics such as D_0, ρ, $(P_0/P)_{c\to 0}$, and $\Gamma_e(q,0)$, the concentration dependences of these quantities are much complicated in nature because they are influenced by the interchain interactions as well as the intrachain interactions. Only a few theories are available at present. Therefore, we discuss briefly the coefficient k_D alone. If we use the volume fraction coefficient k_D^V instead of k_D ($\equiv k_D^V N_A V_H/M$; V_H is the equivalent hydrodynamic volume of the polymer defined by $V_H = 4\pi R_H^3/3$), three theoretical proposals have been presented:

$$k_D^V = 3.2\bar{X}^3 - 1 \quad (Y)^{40} \tag{15}$$

$$k_D^V = \bar{X}^2(8\bar{X} - 6) \quad (AB)^{41,42} \tag{16}$$

$$k_D^V = 8\bar{X}^3 - 7.16 + K \quad (PF)^{43} \tag{17}$$

where the dimensionless parameter $\bar{X}$ is defined by

$$\bar{X} = \bar{S}/R_H \tag{18}$$

The $\bar{S}$ is the radius of equivalent thermodynamic sphere and is defined by A_2 as

$$A_2 = (16\pi N_A/3M^2)\bar{S}^3 \tag{19}$$

The quantity K in eq 17 becomes zero for the good solvent limit. Thus, $\bar{X}$ can be expressed by the well-known penetration function Ψ [$\equiv A_2M^2/(4\pi^{3/2}N_AR_G^3)$] and ρ [$=R_G/R_H$] as

$$\bar{X} = (3\pi^{1/2}/4)^{1/3}\Psi^{1/3}\rho \tag{20}$$

The parameter $\bar{X}$ varies from zero at the Θ-temperature to about unity in the good solvent limit. In Figure 12, these plots of k_D^V vs. $\bar{X}$ are shown in the range $\bar{X} > 0.72$ where the chain is in the good solvent atmosphere; i.e., $k_D^V > 0$. The unfilled data points for PIP in cyclohexane are located well on curve Y (Yamakawa,[40] eq 15), as is the case for PS with $M_w < 4 \times 10^6$ in benzene (filled circles). However, the PS data with $M_w > 4 \times 10^6$ (filled circles with pip) show

a curious molecular weight dependence,[44] $k_D \propto M_w^{0.43}$, and lie in the middle of curves AB (Akcasu–Benmouna) and AB*. The latter curve, k_D^V(AB*), represents k_D^V(AB) − 1. These results induce the question why k_D can be *quantitatively* explained by the theory, e.g., Yamakawa's, though D_0 *cannot*. We have no answer to it at present.

Conclusion

The dynamic properties obtained in dilute solutions of PIP in cyclohexane are considered to represent the universal behavior of highly swollen polymer chains in good solvents. This is due to the high flexibility of PIP chains. Unexplained experimental results hitherto reported for PS in good solvents may be attributed to the lower flexibility of PS chains or to the insufficient chain length of used samples. The dynamic behavior of a highly swollen chain can be fairly well represented by the nondraining Gaussian chain model with nonpreaveraged Oseen hydrodynamic interaction, but not by the pseudo-Gaussian model of Ptitsyn nor the so-called blob model. However, closer inspection of dynamic properties of swollen chains reveals that the real distribution of chain elements in a molecule is significantly distorted from the Gaussian form and is represented by the generalized Domb–Gillis–Wilmers function involving two critical indexes. A 6% difference existing between observed and theoretical Stokes radii may be attributed to the Fixman effect of internal friction.

Acknowledgment. We thank Dr. Kanji Kajiwara for the PIP samples, Sin-ichi Okada for his sedimentation velocity measurements, and Prof. Stockmayer for his timely notice on the significance of Fixman's theory of internal friction.

Appendix

The normalization constant, C_n, for the generalized Domb–Gillis–Wilmers (DGW) distribution function, eq 14, is given as

$$C_n^{-1} = (\sigma_n^{l+1}/t)\Gamma[(l+1)/t] \quad \text{(A.1)}$$

where Γ denotes the gamma function. This function leads to

$$\langle 1/r_n \rangle = \int_0^\infty r^{-1} W(r,n)\, dr = (1/\sigma_n)\{\Gamma(l/t)/\Gamma[(l+1)/t]\} \quad \text{(A.2)}$$

$$\langle r_n^2 \rangle = \sigma_n^2 \Gamma[(l+3)/t]/\Gamma[(l+1)/t] \quad \text{(A.3)}$$

Recent studies of the distribution function $W_{ij}(r,|i-j|)$ for a long, highly swollen, chain molecule indicate that the effect of molecular ends as represented by the i, j dependence of W is negligible for most purposes and the DGW form $W(r,n)$ (with $n \equiv |i-j|$) is applicable to all pairs of chain elements in the molecule (as it is in the case of ring molecule).

Thus, putting

$$\langle r_N^2 \rangle = AN^{2\nu} \qquad \langle r_n^2 \rangle = An^{2\nu} = \langle r_N^2 \rangle (n/N)^{2\nu} \quad \text{(A.4)}$$

and replacing the summation in eq 12 and 13 by integrals, we obtain

$$R_H^{-1} = (2/N^2)\int_0^N (N-n)\langle 1/r_n \rangle\, dn = 2\langle 1/r_N \rangle \int_0^1 (1-x)x^{-\nu}\, dx$$

$$R_H^{-1} = (1/\sigma_N)\{\Gamma(l/t)/\Gamma[(l+1)/t]\}[2/(1-\nu)(2-\nu)] \quad \text{(A.5)}$$

$$R_G^2 = \sigma_N^2\{\Gamma[(l+3)/t]/\Gamma[(l+1)/t]\}/2(1+\nu)(1+2\nu) \quad \text{(A.6)}$$

Hence, we obtain

$$\rho = \{2\Gamma[(l+3)/t]/(1+\nu)(1+2\nu)\Gamma[(l+1)/t]\}^{1/2} \times \{\Gamma(l/t)/(1-\nu)(2-\nu)\Gamma[(l+1)/t]\} \quad \text{(A.7)}$$

This equation gives

ρ = 1.5045 ($t = l = 2$, $\nu = {}^1/_2$); 1.8602 ($t = l = 2$, $\nu = {}^3/_5$); 1.6627 ($t = 2.50$, $l = 2.71$,[31] $\nu = {}^3/_5$); 1.5955 ($t = 2.398$, $l = 2.802$, $\nu = 0.583$)[27] (A.8)

Registry No. Polyisoprene, 9003-31-0.

References and Notes

(1) Han, C. C.; Akcasu, A. Z. *Macromolecules* **1981**, *14*, 1080.
(2) Tsunashima, Y.; Nemoto, N.; Kurata, M. *Macromolecules* **1983**, *16*, 1184.
(3) Nemoto, N.; Makita, Y.; Tsunashima, Y.; Kurata, M. *Macromolecules* **1984**, *17*, 425.
(4) Benmouna, M.; Akcasu, A. Z. *Macromolecules* **1980**, *13*, 409.
(5) ter Meer, H.-U.; Burchard, W.; Wunderlich, W. *Colloid Polym. Sci.* **1980**, *258*, 675.
(6) Kurata, M.; Tsunashima, Y.; Iwama, M.; Kamada, K. *Polymer Handbook*, 2nd ed.; Brandrup, J., Immergut, E. M., Eds.; Wiley: New York, 1975.
(7) Nemoto, N. *Nihon Reoroji Gakkaishi* **1979**, *7*, 3 (in Japanese).
(8) Hadjichristidis, N.; Roovers, J. E. L. *J. Polym. Sci., Polym. Phys. Ed.* **1974**, *12*, 2521.
(9) Kow, C.; Morton, M.; Fetters, L. J.; Hadjichristidis, N. *Rubber Chem. Technol.* **1982**, *55*, 245.
(10) Riddick, J. A.; Bunger, W. B. *Organic Solvents*, 3rd ed.; Wiley-Interscience: New York, 1970.
(11) Hadjichristidis, N.; Fetters, L. J. *J. Polym. Sci., Polym. Phys. Ed.* **1982**, *20*, 2163.
(12) Pike, E. R.; Pomeroy, W. R. M.; Vaughan, J. M. *J. Chem. Phys.* **1975**, *62*, 3188.
(13) Tanaka, Y.; Takeuchi, Y.; Kobayashi, M.; Tadokoro, H. *J. Polym. Sci., Part A-2* **1971**, *9*, 43.
(14) Nemoto, N.; Tsunashima, Y.; Kurata, M. *Polymer J.* **1981**, *13*, 827.
(15) (a) Gulari, E.; Gulari, E.; Tsunashima, Y.; Chu, B. *J. Chem. Phys.* **1979**, *70*, 3965. (b) Tsunashima, Y.; Nemoto, N.; Makita, Y.; Kurata, M. *Bull. Inst. Chem. Res., Kyoto Univ.* **1980**, *59*, 293.
(16) Burchard, W.; Schmidt, M.; Stockmayer, W. H. *Macromolecules* **1980**, *13*, 580.
(17) Billick, I. H. *J. Phys. Chem.* **1962**, *66*, 565.
(18) Fujita, H. *Mathematical Theory of Sedimentation Analysis*; Academic: New York, 1962; Chapter II. See also: Fujita, H. *Foundation of Ultracentrifugal Analysis*; Wiley-Interscience: New York, 1975; Chapter V.
(19) Blair, J. E.; Williams, J. W. *J. Phys. Chem.* **1964**, *68*, 161.
(20) Abe, M.; Sakato, K.; Kageyama, T.; Fukatsu, M.; Kurata, M. *Bull. Chem. Soc. Jpn.* **1968**, *41*, 2330.
(21) Altgelt, K.; Schultz, G. V. *Makromol. Chem.* **1959**, *32*, 66.
(22) As indicated in Table I, the cis contents of higher molecular weight samples, L-11 and L-16, are higher (=trans being lower) than those of the others. These differences go beyond uncertainties in the estimation of the microstructure and may be responsible to the higher exponent, $\nu_{R_G} = 0.61$, than the theoretical value by 0.01. According to Chaturvedi and Patel (*J. Polym. Sci., Polym. Phys. Ed.* **1985**, *23*, 1255), however, R_G for *trans*-PIP (98% trans-1,4) in cyclohexane at 30 °C has weaker molecular weight dependence [R_G(trans) $\approx 4 \times 10^{-9} M_w^{0.54}$ (cm)] and becomes comparable with R_G of our samples of high cis contents in $30 < M_w \times 10^{-5} < 70$. This indicates that if the cis contents of L-11 and L-16 were about 70%, similar to those of L-14, L-12, and L-15, the values of R_G might become a little bit smaller than those listed in Table I. It is thus conceivable that the experimentally plausible exponent ν_{R_G} might go down from 0.61 to a smaller value, say about 0.59.
(23) Utiyama, H.; Utsumi, S.; Tsunashima, Y.; Kurata, M. *Macromolecules* **1978**, *11*, 506.
(24) Miyaki, Y.; Einaga, Y.; Fujita, H. *Macromolecules* **1978**, *11*, 1180.
(25) Kirkwood, J. G. *J. Polymer Sci.* **1954**, *12*, 1.
(26) Akcasu, A. G.; Gurol, H. *J. Polym. Sci., Polym. Phys. Ed.* **1976**, *14*, 1.
(27) Tsunashima, Y.; Kurata, M. *J. Chem. Phys.* **1986**, *84*, 6432.
(28) Domb, C.; Gillis, J.; Wilmers, G. *Prog. Phys. Soc. (London)* **1965**, *85*, 625.
(29) Stockmayer, W. H.; Hammouda, B. *Pure Appl. Chem.* **1984**, *56*, 1373. See also ref 2 and: Schmidt, M.; Burchard, W. *Macromolecules 14*, **1981**, 210.
(30) Fixman, M. *J. Chem. Phys.* **1986**, *84*, 4085.
(31) des Cloiseaux, J. *J. Phys. (Les Ulis, Fr.)* **1980**, *41*, 223.

(32) Bantle, S.; Schmidt, M.; Burchard, W. *Macromolecules* **1982**, *15*, 1604.
(33) Tanaka, G.; Stockmayer, W. H. *Proc. Natl. Acad. Sci.* **1982**, *79*, 6401.
(34) Akcasu, A. Z.; Benmouna, M.; Han, C. C. *Polymer* **1980**, *21*, 866.
(35) Utiyama, H.; Tsunashima, Y.; Kurata, M. *J. Chem. Phys.* **1971**, *55*, 3133. See for example, Figure 11.
(36) Benmouna, M.; Akcasu, A. Z. *Macromolecules* **1978**, *11*, 1187.
(37) Oono, Y. *Adv. Chem. Phys.*, in press. Oono, Y., private communication. Here our PS data (ref 3) have been misplotted in his Figure 24. In addition, his value of $\rho = 1.562$ should be revised as 1.514 because there are simple mathematical errors.
(38) Perico, A.; Piaggio, P.; Cuniberti, C. *J. Chem. Phys.* **1975**, *62*, 2690.
(39) Tsunashima, Y.; Nemoto, N.; Kurata, M. *Macromolecules* **1983**, *16*, 584.
(40) Yamakawa, H. *J. Chem. Phys.* **1962**, *36*, 2995.
(41) Akcasu, A. Z.; Benmouna, M. *Macromolecules* **1978**, *11*, 1193.
(42) Akcasu, A. Z. *Polymer* **1981**, *22*, 1169.
(43) Pyun, C. W.; Fixman, M. *J. Chem. Phys.* **1964**, *41*, 937.
(44) Tsunashima, Y.; Nemoto, N. *Macromolecules* **1984**, *17*, 2931.

A Computer Simulation for the Aggregation of Associating Polymers

Anna C. Balazs,† Charles Anderson,‡ and M. Muthukumar*

Polymer Science and Engineering Department, University of Massachusetts, Amherst, Massachusetts 01003. *Received October 30, 1986*

ABSTRACT: A computer simulation (in 2-D) is used to model the aggregation process for self-avoiding flexible polymers which contain two "stickers", one at each chain end. We assume that the strong attractive interaction between these end sites leads the chains to aggregate and form clusters. By assuming that the monomer concentration of our aggregate is comparable to the monomer concentration at the overlap threshold for a solution of 2-D self-avoiding random walk chains, we have been able to correlate the radius of gyration for the cluster to n and N, the degree of polymerization and the number of chains, respectively. We find that $R_g \sim N^{1/2}n^{3/4}$. However, the presence of self-loops causes the cluster to contract in size and results in a small deviation from the predicted exponent relating R_g and N. We also demonstrate that the diffusion-limited network formation studied here is distinctly different from the small-particle diffusion limited aggregation.

Associating polymers are flexible macromolecules which contain a number of sites that strongly attract each other. The strong interaction between these sites leads the chains to aggregate and form clusters. This, in turn, gives rise to a variety of unusual physical properties.[1-6] Of particular interest are polymers in which the associating sites or "stickers" are located at the ends of the chains.[7,8] This feature is relevant in several self-assembling processes, such as the aggregation of telechelic ionomers,[9] mesophase formation in didiscotic liquid crystals,[10] and gel formation,[11] as well as the formation of microemulsions[12] and block copolymers. While there is considerable experimental evidence for the end-to-end association in the systems listed above, the exact size, shape, and number of stickers involved in these structures remain uncertain.[3]

In an attempt to understand the details of structures underlying these processes, we present below a computer simulation in two dimensions to model the aggregation process for flexible chains which contain two stickers, one at each chain end. In general, one of the key features in the above-mentioned processes is the lifetime of the association of the stickers.[13] This lifetime depends strongly on the chemical nature of the stickers. The computer simulation of such reversible associations of polymer chains with stickers is a very difficult task in terms of the necessary computer time. As a start, we consider only the case where the lifetime of the association is longer than the relaxation time of the individual chain and the characteristic time for the diffusion of a chain inside the aggregate. Consequently, we assume that the chains aggregate by a given end of a chain sticking irreversibly to either the other end of the same chain or an end of a different chain. Attention is focused only on the formation of a single aggregate.

The advantage afforded by this computer simulation is that it yields both a qualitative and quantitative means of understanding the factors which influence the size and shape of the growing cluster. First, the figures generated via this method allow us to actually visualize the growth and changes in the aggregate. Second, various features of the cluster, such as the radius of gyration or the number of intra- and inter-chain interactions are easily computed. Third, "experiments" to alter various polymer properties (such as chain length) are easily carried out, and hence we can examine how such variations affect the aggregation process. Finally, the procedure used here is similar to that used to study the class of problems known as diffusion-limited aggregation (DLA).[14] In these problems, diffusion of the particles to the surface of the aggregate is the rate-limiting step. As is common in this class of calculations, we will search for a scaling law that describes the evolution of the cluster.

The Model

The simulation is started by placing a seed chain, of specified length but with self-avoiding random configuration, at the center of a two-dimensional square lattice. The chain is taken to be composed of $(n - 1)$ bonds. All chains in the simulation obey the excluded volume criteria, in that no lattice site is permitted to be doubly occupied. The last bond at both ends of the chain is designated as a "tail". The configuration of the first chain remains fixed. Another chain of equal length is introduced and allowed to execute a self-avoiding random walk. In this paper we consider two limits which we call dilute and concentrated.

† Present address: Department of Materials Science and Engineering, University of Pittsburgh, Pittsburgh, PA 15261.
‡ Present address: GTE Laboratories, Waltham, MA 02254.

0024-9297/87/2220-1999$01.50/0